Modeling and Analysis of a Low Pressure Fuel Cell System

R. Tirnovan*, A. Miraoui**, R. Munteanu*, I. Vadan*, H. Balan*
* Electrical Engineering Department, Technical University of Cluj-Napoca (TUCN), ROMANIA
**Control Systems Department (GSC), University of Technology of Belfort-Montbéliard (UTBM) FRANCE

Abstract: **- This paper presents a study of the fuel cell system performance operating at low pressure and different temperature levels. A polymer electrolyte fuel cell (PEFC) is analyzed according with the possibility of using in transport applications. Therefore, it begin with the description of a parametric model of the fuel cell which has been developed using a combination between empirical and mathematics modeling techniques. This model enables to study the influence of the gases management (pressure) on the fuel cell stack performances. The study continues with the modeling and simulation of a blower as the active element for the compression air system.**

I INTRODUCTION

Air pollution is a serious problem, which affects many countries, especially in densely populated cities and highly polluting engine vehicles. Non-polluting energy carrier has been driving during the last few years. Fuel cell systems (FC) have been showing as an alternative to the classic power sources due their efficiency, low aggression to the environment, reliability, applications, and performances. Electric vehicles represent attractive applications where fuel cells could be used successfully.

A fuel cell vehicle would be better to four-stroke engine or electric battery-powered vehicles, by offering both zero tail pipe emissions and combustion and the same class range. Unlike 50kW automobile-sized fuel cell stacks, the vehicular 5kW fuel cell has not received much attention.

Sir William Grove discovered the principle behind fuel cells as early as 1839. However, due to high costs, the technology was not significantly used until the American Gemini space missions of the 1960's. A fuel cell produces electrochemical energy (electric and thermal) due to the passage hydrogen through an anode and oxygen (or air) through a cathode. The exchange of electrical charges (ions) is facilitated by an electrolyte placed between the anode and cathode. The ion flow through the electrolyte produces an electrical current in an external circuit or load. Any hydrocarbon material, in principle, can be used as fuel independently of being gas, liquid or solid.

At this time, the principal fuel cell technologies, developed to equip vehicles, are the PEFC (Polymer Electrolyte Fuel Cell), the AFC (Alkaline Fuel Cell) and the SOFC (Solid Oxide Fuel Cell) [1, 2]. The dimensioning of these stacks will be strongly depending on the architecture of the power generating unit and hybridization considered (if it is necessary).

PEFC could be a great alternative to replace the traditional distributed power sources and especially in automotive applications. They operate at low temperatures providing a fast start-up and produce water as by-product waste. The electrolyte, which is a solid polymer, allows a reduced and compact construction.

A fuel cell needs to be associated with auxiliaries who must ensure essential functions as to convey the reactants, to evacuate the products and to manage the temperature of the stack. These auxiliaries are generally electrical consumers, and must be considered as parasites charges, which influence directly the electrical energy delivered by the stack. Thus, a reduction of net electrical power, delivered to the consumer, is the consequences of these parasites.

One can distinguish different types of fuel cell systems classified by:

- the level of the pressure they work (it gives the sizing of the air compressor);
- the fuel nature: hydrogen stored under liquid or gas form, hydrogen stored in the form of hydride, fuel to reform (generally a hydrocarbon or an alcohol which one extracts hydrogen by a reforming operation – these materials have to pass through a reformer to liberate the hydrogen of the carbon).

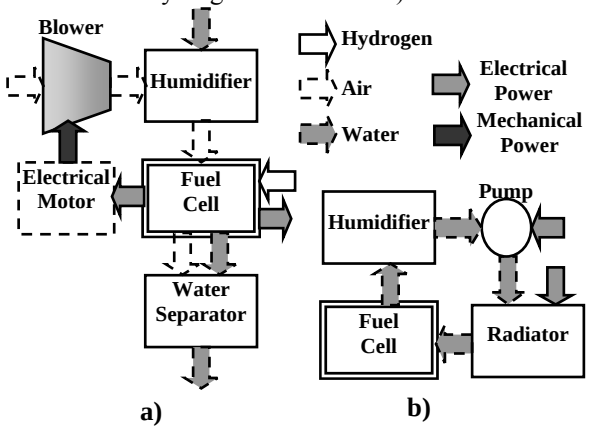

Fig.1. Fuel cell system diagram: a) air system; b) coolant loop.

The natural gas, for example, is reformed through vapors at high temperatures. A similar process, called gasification, is applied to coal, biomass and to a wide range of hydrocarbon residues [1, 2]. The architecture of the power-generating unit will be also strongly dependent on the auxiliaries. The performances of a system are generally given compared to their specific powers or power per volume, but also in terms of output. A single cell, under normal operation, typically allows 0.5V to 0.9V between the two electrodes. For use in energy generation systems, where a relatively high power is needed, several cells are connected in series, arranging a stack that can supply hundreds of kilowatts.

Overall, fuel cell system consists of a combustible circuit, a combustive circuit and a loop of cooling. Sometimes, a humidification system is needed to complete this unit. It can be coupled with the loop of cooling or it can operate independently (Fig.1).

Other way the components of a fuel cell system can to be segmented in three subsystems as is shown in Table I.

Therefore, choosing an optimal solution, architecture of a fuel cell system imposes the analysis of the application and all the fuel cell subsystems. To obtain good performances the modeling, simulation of all components and subsystems, consequently of the complete fuel cell system is recommended. First, the modeling and simulation of "the fuel cell subsystem" must be done highlighting the influence of each component.

II Basic Fuel Cell Operation

An element of fuel cell carries out the direct transformation of the chemical energy of a reaction (in fact the change in the free Gibbs energy of reaction ΔG) into electric power according to the equation (electrochemical balance) [3]:

$$\Delta G + nF \cdot E_{eq} = 0 \quad where\ \Delta G < 0\ , \qquad (1)$$

with:

- E_{eq} – e.m.f (electromotive force) of the stack to balance (i.e. null intensity of the current I);
- n – the number of electrons exchanged in the elementary electrochemical reactions (reactions of half pile);
- F = 96500 C = 1 Faraday – i.e. quantity of electricity associated with a mole of electrons.

TABLE I
Fuel Cells System Components

Fuel Processor Sub-System		Fuel Cell Sub-System	Balance-of-Plant
Reformer Generator ▪ ATR ▪ HTS ▪ Sulfur removal ▪ LTS ▪ Steam generator ▪ Air preaheter ▪ Steam superheater ▪ Reformer humidifier	Fuel Supply ▪ Fuel pump ▪ Fuel vaporizer	▪ Fuel Cell Stack (Unit Cells) ▪ Stack Hardware ▪ Fuel Cell Heat Exchanger ▪ Compressor/Expander ▪ Anode Tailgas Burner ▪ Sensors & Control Valves	▪ Start-up Battery ▪ System Controller ▪ System Packaging ▪ Electrical ▪ Safety
Reformer Conditioner ▪ NH_3 removal ▪ PROX ▪ Anode gas cooler ▪ Economizers ▪ Anode inlet knockout drum	Water Supply ▪ Water separators ▪ Heat exchanger ▪ Steam drum ▪ Process water reservoir		
Sensors & Control Valves for each section			

In the case of the hydrogen/oxygen stack (Fig.2), the total chemical reaction, associated with this transformation, is the combustion of hydrogen in oxygen:

$$H_2 + \frac{1}{2} O_2 \rightarrow H_2O\ . \qquad (2)$$

It corresponds, for standard conditions, with an e.m.f. to the balance at 25 °C:

$$E_{eq}^0 = -\frac{\Delta G^0}{nF} = \frac{237 \times 10^3}{2 \times 96\ 500} = 1.229\,V\ . \qquad (3)$$

The electrochemical oxidation of hydrogen is realized to the anode, made of a conducting catalytic material, constituting the negative pole of the stack. For an acid electrolyte (perfluorosulfonic acid polymer), it can be written:

$$H_2 \rightarrow 2H^+ + 2e^-\ ; \qquad (4)$$

while the electrochemical reduction of oxygen occurs with a catalytic cathode, constituting the positive pole of the cell:

$$\frac{1}{2} O_2 + 2H^+ + 2e^- \rightarrow H_2O\ . \qquad (5)$$

The reactions (4) and (5), which bring into play a transfer of load (electrons) at the interface between electrode and electrolyte, are called electrochemical reactions.

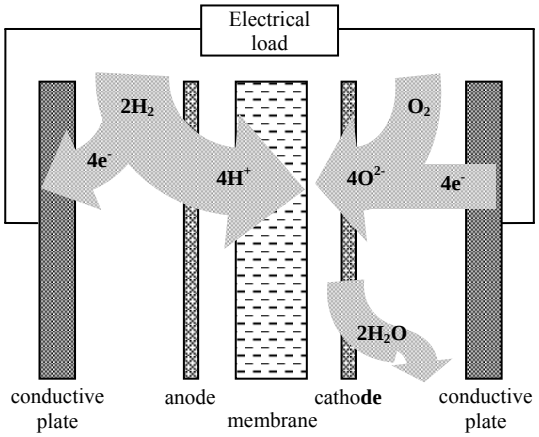

Fig.2. Basic PEFC operation.

The two compartments, anodic and cathodic, are separated by an ionic driver, the electrolyte, and/or a membrane preventing the reactants from mixing and the electrons to cross the heart of the stack. The e.m.f. stack E is equal to the difference of the potentials of electrode (index "c" for cathode and "a" for anode), that is to say:

$$E = E_c^+ - E_a^- \text{ ,} \tag{6}$$

The results of the electrochemical reactions are: water, heat and electrical energy.

III Fuel Cell Model Formulation

A. Fuel cell reversible voltage

In this paper, a semi-empirical approach is adopted for fuel cell modeling. One considers that the model of the fuel cell stack can be obtained by multiplying one cell model with the number of the cell. The potential characteristic that means the output voltage as current (current density), of a single cell can be defined by the following expression [1, , 4]:

$$v(j) = v_{rev} - v_{ohmic} - v_{act} - v_{con} \text{ ,} \tag{7}$$

where:

- v_{rev} represents the reversible voltage (the thermodynamic potential of the cell);
- V_{ohmic} is the ohmic voltage drop (ohmic voltage drop resulting from the resistances of the conduction protons through the membrane and of the electrons through the electrical circuit);
- v_{act} is the activation over potential or the voltage drop due to the activation of the anode and cathode (a measure of the voltage associated with the electrodes);
- v_{con} is the voltage drop, which results from the reduction in concentration of the reactants gases, or from the transport of mass of oxygen and hydrogen.

For an electrochemical reaction [1],

$$A + ne^- \Leftrightarrow B \text{ ,} \tag{8}$$

where A and B are the reacting species, the law of Nernst calculates the potential of electrode:

$$v_{A/B} = E^0_{A/B} + \frac{RT}{nF} ln\left(\frac{a_A}{a_B}\right) \text{ ,} \tag{9}$$

with:

- $E^0_{A/B}$ (V) - the standard potential (by definition it is measured by comparing to the standard electrode with hydrogen ESH, of null potential of the electrode, at 25°C);
- a_A, a_B – the activities of A and B;
- R=8.3145 J/(K·mol) – the universal constant of gases;
- T is the absolute temperature.

One can write:

$$v_{rev} = 1.229 - 0.85\times10^{-3}\left(T - T_{ref}\right) + \\ + 4.31\times10^{-5} T\left[ln\left(p_{H_2}\right) + \frac{1}{2} ln\left(p_{O_2}\right)\right] \text{ (V),} \tag{10}$$

where:

- T_{ref} is the absolute reference of temperature (in our study 298.15 K);
- p_{H_2}, p_{O_2} are the interfacial hydrogen and the oxygen partial pressures, (atm) [4].

In this paper, we made an approximation, replacing the interfacial partial pressures with the effective partial pressures (exponent avg) in the flow channels using the relations below [4]:

$$p_{O_2} = p_{O_2}^{avg} = \frac{p_{O_{2,in}} - p_{O_{2,out}}}{ln\left(\frac{p_{O_{2,in}}}{p_{O_{2,out}}}\right)} (atm) \text{ ,} \tag{11}$$

$$p_{H_2} = p_{H_2}^{avg} = \frac{p_{H_{2,in}} - p_{H_{2,out}}}{2} (atm) \text{ ,} \tag{12}$$

the indexes *in* and *out* denote the inlet and outlet partial pressures value. If s_O is stoichiometric ratio of oxygen and 0.21 is the value of the molar fraction of oxygen in dry air (relative humidity RH=0), then (11) becomes:

$$p_{O_2} = \frac{0.21/s_O}{ln\left(\frac{s_O}{s_O - 1}\right)}\left(p_{air,in} - p_{vap}\right)(atm) \text{ .} \tag{13}$$

In (13) $p_{air,in}=p_{in}$ is the inlet humidified air and $p_{vap}=(RH/100)\cdot p_{sat}$ is the partial pressure of the water vapour at the cathode. One takes into account the saturation case (RH=100 %) when the vapors pressure is equal to the saturation pressure p_{sat}, which is a function only of temperature):

$$p_{sat} = \frac{e^{\left[23.1961 - 3816.44/(T - 46.13)\right]}}{101325} (atm) \text{ .} \tag{14}$$

The hydrogen partial pressure (anode) is imposed by the membrane mechanical constraint (the maximum value of the pressure drop between cathode and anode approximately 0.3 atm to avoid membrane fracture) and anode relative humidity 50%:

$$p_{H_2} = p_{in} - 0.5 p_{sat}\ (atm). \tag{15}$$

B. Fuel cell activation voltage

In this paper, for over potential activation voltage computing, the following expression was considered:

$$v_{act} = v_{act,1} + v_{act,2}, \tag{16}$$

where $v_{act,1}$=VACT1·ln(j) and $v_{act,2}$ is a correction term with temperature and oxygen partial pressure.

C. Fuel cell concentration drop voltage

A decrease of the partial pressures of the reactant gases, along the flow channels, takes place. It is the result of the mass transport, which affects the concentrations of hydrogen and oxygen. The reduction of oxygen and hydrogen pressures depends on the electrical current and the physical characteristics of the system. The following expression, given in [5], has been used to compute the concentration over potential:

$$v_{conc} = -VCONC \cdot ln\left(1 - \frac{j}{J_{max}}\right). \tag{17}$$

J_{max} is defined as the value of the current density when the reactants concentrations become null. It depends on temperature and operating pressures. Typical values for J_{max} are in the range of 0.5A/cm² to 1.5A/cm^2. The coefficient VCONC depends on the cell and its operation state.

Therefore, our model has five degrees of freedom. The five parameters (ρ_C, VACT1, $v_{act,2}$, J_{max} and VCONC) have to be determined fitting the modeling curve to the experimental data, and their expressions follow the model below:

$$\begin{aligned} F(T, p_{O_2}) = {} & F_{00}(1,1) + F_{01}(1,2)\cdot T + \\ & + \left[F_{10}(2,1) + F_{11}(2,2)\cdot T\right]\cdot p_{O_2} + \\ & + \left[F_{20}(3,1) + F_{21}(3,2)\cdot T\right]\cdot p_{O_2}^2 \end{aligned} \tag{18}$$

The influence of the hydrogen partial pressure can be neglected as long as the hydrogen fraction on the anodic side is greater than 20% [6]. Consequently, the five parameters depend on the cell temperature and the oxygen partial pressure only.

IV Pressure Impact On Fuel Cell Performance

Current technologies allow PEFC operation at pressures between 1atm and 5atm. The studies presented in open literature show that important changes in fuel cell characteristic take place between 1atm and 3atm [7,8].

Higher pressures than 3atm produce smaller and smaller changes. Also one can remark that the power density, function of stack temperature (between 50°C and 80°C to 85°C) and operating pressure, ranges between 0.25A/cm^2 and 0.6W/cm² to 0.7W/cm^2 [1,4,7,9].

The beneficial effects operating at high pressure on fuel cell performance can be summarized in the increase of power density, the decreasing of the fuel stack volume/mass, and explained because [2]:

- the increasing of reactant partial pressure;
- gas solubility, and mass transfer rates are higher;
- easier water evacuation;
- increased pressure also tends to increase system efficiencies.

However, one can make few remarks through the cost of high pressure operating [2]:

- there are compromises such as thicker piping and additional expense for pressurization;
- the increasing of parasitic power cost;
- the increasing of hardware and materials problems and cost;
- the pressure differentials must be minimized to prevent reactant gas leakage through the electrolyte and seals.

So, a balance solution between the benefits of increased pressure and hardware and materials problems must be adopted. In this paragraph, we tried to make a short analysis of the operating pressure of the fuel cell. The question is if one can make delimitation between the applications, which lend to high-pressure operation (involving an air compressor) and the low-pressure operation (involving a blower).

A. Pressure losses in laminar flow through serpentine channels

As was illustrated in Fig.3, an elementary PEFC (planar architecture) consists of two porous electrodes separated by a polymer membrane permeable only for protons. The reactants are distributed through the electrodes and membrane from two distributor plates. The gases are forced through channels etched in the plates. The channels can be of different patterns, i.e., parallel, single serpentine, parallel serpentine or interdigitated channels [10].

Typically, the channel sizes and the gas flow rates are small and the flow is expected to be laminar. The pressure losses in the flow distributor plate depend on the Reynolds number and geometric parameters of the small flow channels.

Reynolds number can be expressed by:

$$Re = \frac{D \cdot V \cdot \rho}{\mu} = \frac{D \cdot G}{\mu}, \tag{19}$$

where:

- D is the characteristic length (m);
- G is the mass velocity (kg/s);
- μ is the dynamic (absolute) viscosity (kg/(m·s));
- ρ is the density (kg/m^3);
- V is the fluid velocity (m/s).

The study [10] permits an evaluation of pressure losses in channels. It considers the case of a serpentine channel with a total length of 250mm and containing five straight channels of 50mm length connected by four 180° bends..

One can say that it correspond to a 10cm^2 active surface. The pressure drops over a range of mass flow rates was computed (Table II).

TABLE II
PRESSURE DROP

Re	p(Pa)
100	2.03×10^2
212	4.73×10^2
424	1.10×10^3
706	2.13×10^3

If we assume a power density equal 0.25W/cm^2, a 10 cm^2 of active surface of fuel single cell will produce 2.5W. One can compute the mass flow of air request for initial conditions 1atm pressure, 70°C temperature, a relative humidity of 100%, stoichiometric ratio 2.5 and 0.7A/cm^2 current density. We obtained 6.3×10^{-3} g/s for air mass flow and 5.32×10^{-6} m^3/s for the volumetric flow. For a channels section about 4mm^2, the fluid velocity will be approximatively 1.33m/s. Reynolds number is 155 which is in correspondence with a pressure drop Δp about 336Pa (Table II).

If the same algorithm is applied for a power density of 0.6W/cm^2 (1A/cm^2 current density) the results are the followings: Re=337 – which corresponds for a pressure drop about 840Pa. For a 400 cm^2 it results about 30000Pa to 40000Pa.

Therefore, operating at high pressures presumes an increase of the drop pressure in channels, which must be supported by the compression air system.

B. Parasitic losses due to the compression air system

Parasitic losses are electric power consumption needed to assure the operation of the auxiliary fuel cell subsystems. Generally, the compression power can be computed with.

$$P_{cp} = \frac{w_{air} \cdot T_{air} \cdot C_p}{\eta_{cp}} \cdot \left[\left(\frac{p_{out}}{p_{in}} \right)^{\frac{\gamma-1}{\gamma}} - 1 \right] \text{(W)}, \quad (20)$$

where:

- η_{cp} is the compression efficiency (between 0.6-0.7 for a turbo compressor and 0.3-0.4 for a blower);
- C_p the specific heat capacity of the gas;
- W_{air}, T_{air}, the mass flow and absolute temperature of the air;
- p_{in}, p_{out} are the inlet and outlet pressure of the gas.

Figure 3 illustrates the fuel cell net power density for the two cases: blower and compressor. For low power density, operating to low or high pressure, offers the same benefits.

Operate at low pressure balances the ratio between price of compression subsystem and performance for low density fuel cells stack (i.e. a 5kW stack which can equip a scooter).

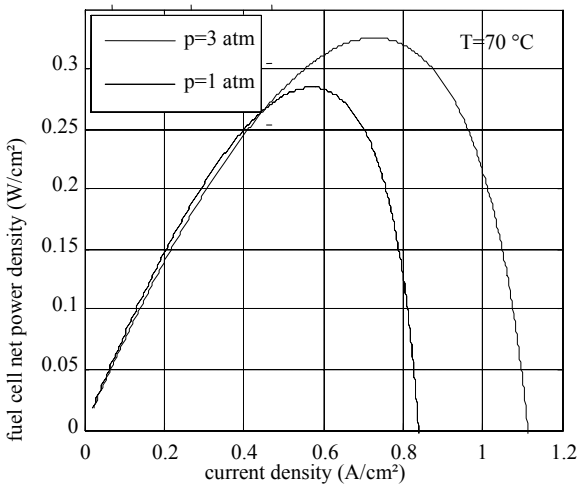

Fig.3. Fuel cell net power density for two different air pressures:

V. BLOWER MODELING

The structure of the fuel cell system, which is analyzed in the paper, is shown in figure 1.

A compressor is an expensive device, which operates at a very high speed around 100 kRPM. It makes one wonder if it would not be better to use a blower as supply air device. It is cheaper and slower than a turbo compressor and needs a lower power supply at the same flow rate (even is efficiency is lower). A simple blower operates at low pressure, close to the atmospheric pressure, and at low speed about few thousands RPM [11].

A. Physical laws for blower applications [12, 13]

A particularly useful concept for the user is the difference of the total pressures between the enter and the exit of the blower:

$$\Delta p = p_{out} - p_{in} . \quad (21)$$

In the case of the blowers, which heat very little, it is not necessary to distinguish between the adiabatic and isothermal machines. For the compression power, one has quite simply the relation:

$$P_{bl} = \frac{w_{air}}{\eta_{bl} \cdot \rho_{air}} \left(p_{out} - p_{in} \right) \cdot 101325 \text{ (W)}, \quad (22)$$

with 'bl' the index for blower.

B. The basic fan laws chart [12, 13]

One can define the principle physical quantities, which characterized the blower operation, such as the volume (flow), pressure and power.

The specific relationship between these quantities and the rotation speed or gas characteristics can be summarized in:

- The mass flow changes in direct ratio to the speed N (rot/min):

$$w_2 = w_1\left(\frac{N_2}{N_1}\right) \text{ (kg/s)}; \quad (23)$$

- The pressure changes as the square of the speed ratio:

$$\Delta p_2 = \Delta p_1\left(\frac{N_2}{N_1}\right)^2 \text{ (atm)}; \quad (24)$$

- The compression power changes as the cube of the speed ratio:

$$P_2 = P_1\left(\frac{N_2}{N_1}\right)^3 \text{ (W)}; \quad (25)$$

- Pressure varies in direct proportion to the density ratio D:

$$\Delta p_2 = \Delta p_1\left(\frac{D_2}{D_1}\right) \text{(atm)}; \quad (26)$$

- the change of the power with the ratio density. The power varies in direct proportion to the specific gravity (ratio of density of gas to density of air):

$$P_2 = P_1\left(\frac{D_2}{D_1}\right) \text{(W)}. \quad (27)$$

C. Blower map fitting

The blowers operate at low pressure and average or high values of the mass flow. If one computes the maximum value of the airflow needs to assure a good supply for a fuel cell, the relations are:

$$p_{vap} = RH \cdot p_{sat} \text{ (atm)}; \quad (28)$$

$$p_{dry\_air} = p_{air} - p_{vap} \text{ (atm)}; \quad (29)$$

$$\omega = \frac{M_{vap}}{M_{dry\_air}} \cdot \frac{p_{vap}}{p_{dry\_air}} \quad (30)$$

$$y_{O_2} = \frac{x_{O_2} \cdot M_{O_2}}{x_{O_2} \cdot M_{O_2} + (1 - x_{O_2}) \cdot M_{N_2}} \quad (31)$$

$$w_{dry\_air} = \frac{w_{O_2}}{y_{O_2}} \text{ (kg/s)}; \quad (32)$$

$$w_{O_2} = s_{O_2} \cdot w_{O_2,r} \text{ (kg/s)}; \quad (33)$$

$$w_{O_2,r} = \frac{M_{O_2} \cdot n \cdot A \cdot j}{4F} \text{ (kg/s)}; \quad (34)$$

$$w_{air} = (1 + \omega) \cdot w_{dry\_air} \text{ (kg/s)}; \quad (35)$$

$$w_{vap} = w_{air} - w_{dry\_air} \text{ (kg/s)}; \quad (36)$$

$$\rho_{air} = \left(\frac{p_{dry\_air}}{R_{dry\_air} \cdot T} + \frac{p_{vap}}{R_{vap} \cdot T}\right) \cdot 101325 \text{ (kg/m}^3\text{)} \quad (37)$$

$$D_{air} = \frac{w_{air}}{\rho_{air}} \text{ (m}^3\text{/s)}, \quad (38)$$

where:

- p_{vap} – the vapors partial pressure;
- p_{sat} – the pressure of the saturated vapors;
- p_{air} – the pressure of the humidify of inlet air;
- p_{dry_air} is the partial pressure of the dry inlet air;
- ω – the humidity ratio;
- y_{O2} – the oxygen mass fraction;
- x_{O2} – dry air oxygen mole fraction (0.21);
- M_{O2}, M_{N2}, M_{vap}, M_{dry_air} are the molar mass (kg/mol) of the oxygen, nitrogen, water vapors respectively of the dry air;
- $w_{O2,r}$, w_{O2}, w_{vap}, w_{dry_air}, w_{air} are the mass flow of the reacted oxygen, oxygen request, water vapors, dry air respectively of the air request;
- A – active area (cm^2);
- j – current density (A/cm^2);
- n – cells number;
- s – stoichiometric ratio;
- D_{air} – volumetric flow of the air;
- R_{dry_air} =287.05 J/(kg·K) gas constant for dry air;
- R_{vap} = 461.495 J/(kg·K) gas constant for vapors.

For a 5 kW fuel cell (RH=50%, T_{air}=298.15 K, A=320 cm^2, n=50, j=0.65 A/cm^2, s=2) the maximum mass air flow is w_{dry_air}=7.5 g/s. Same time for a 20 kW fuel cell we obtain is w_{dry_air}=14.9 g/s and for a 40 kW fuel cell is w_{dry_air}=56 g/s. So, one can choose for existing blowers that which satisfy this opportunity.

Indeed, observation of the blower map chosen [13] shows that a relationship of the following type [11]:

$$\begin{cases} \Delta p = \sum_{k=0}^{2} A_k \cdot w^k, \\ A_k = \sum_{i=0}^{2} a_{ki} \cdot N^i, \end{cases} \quad (39)$$

can be used for the blower map fitting.

For the operating line, we used a square approximation:

$$\Delta p = \sum_{j=0}^{2} B_j \cdot w^j. \quad (40)$$

The results of the curves fitting are shown in figure 4. a,b,c (AMETEK, Tech. Bulletin, BLDC Bypass Blower,

1166340M, 6632 M, 116637 M) and indicate a good approximation of the measured values.

In addition, in the figure 4 it is indicate the operating line for each blower.

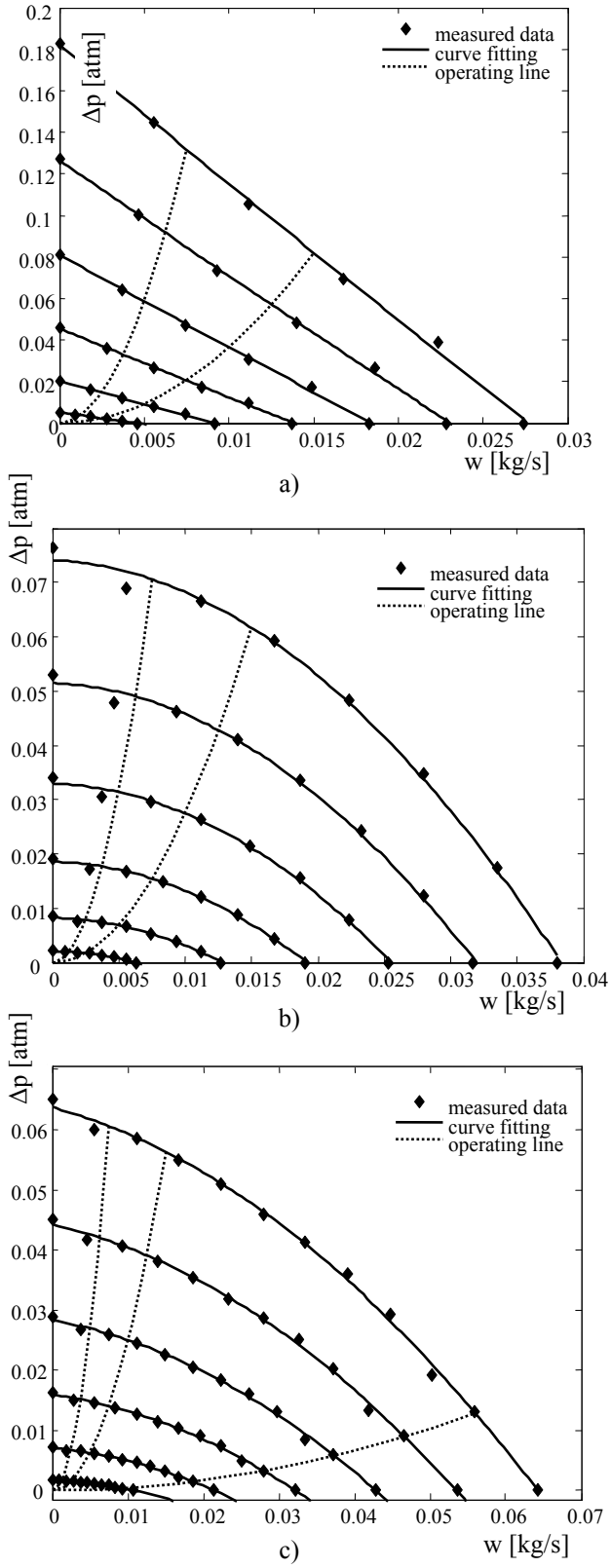

Fig. 4. Blower map fitting [15]:
a) BLDC250 116632; b) BLDC250 116634; c) BLBC250 116637.

VI. Dynamic Of Low Pressure Fuel Cell Air Supply System (Open Loop)

The analysis started by assuming the following suppositions:

- the hydrogen supply is very well controlled. The flow rate can be very fast adjusted, following the air pressure, to provide minimum pressure difference across the membrane (the anode pressure is equal to cathode pressure);
- in our model we ignored the heat transfer effects and we considered the temperature of the reactant flows and fuel cell stack are assumed constant at 70°C;
- the relative humidity of the stack inlet hydrogen and airflow is assumed to be 100%.

We have considered a fuel stack with a maximum power about 5 kW, with 50 cells at 0.45 V/cell, 320 cm^2 /cell active, which consume about 7.5 g/s of air at 0.6 A/cm^2 current density. It means a maximum stack power equal to 0.6·0.45·50·320=4320 W. The blower is sized so that the excess of the oxygen ratio s (stoichiometric ratio) is equal to 2 that mean an air excess ratio s=2, and the hydrogen stoichiometric ratio is 1.5. The BLDC250/116632 model was used in the simulation.

The dynamic model of the blower can be described by

$$J_{bl}\frac{d\Omega_{bl}}{dt}=\left(\tau_m-\tau_{cp}\right), \tag{41}$$

with:

- J_{bl} ($kg\cdot m^2$) is the total inertia of the blower and the driving motor;
- Ω_{bl} (rad/s) is the blower speed;
- τ_m (N·m) is the blower driving motor torque;
- τ_{cp} (N·m) is the torque required for the compression.

The blower motor torque was computed using a static motor equation:

$$\tau_m=\frac{\eta_m\cdot k_t}{R_m}\left(v_m-k_v\cdot\Omega_{bl}\right), \tag{42}$$

where

- k_t is the motor torque constant (N·m/A);
- k_v is the voltage motor constant (V/(rad ·s));
- R_m (ohm) – the motor resistance;
- v_m (V) is the reference supply voltage;
- η_m is the motor efficiency.

The torque required for the compression was obtained with

$$\tau_{cp}=\frac{P_{bl}}{\eta_{cp}\cdot\Omega_{bl}}, \tag{43}$$

where η_{cp} is the compression efficiency and the power P_{bl} is computed with (24).

The simulation results are shown in Fig. 5.

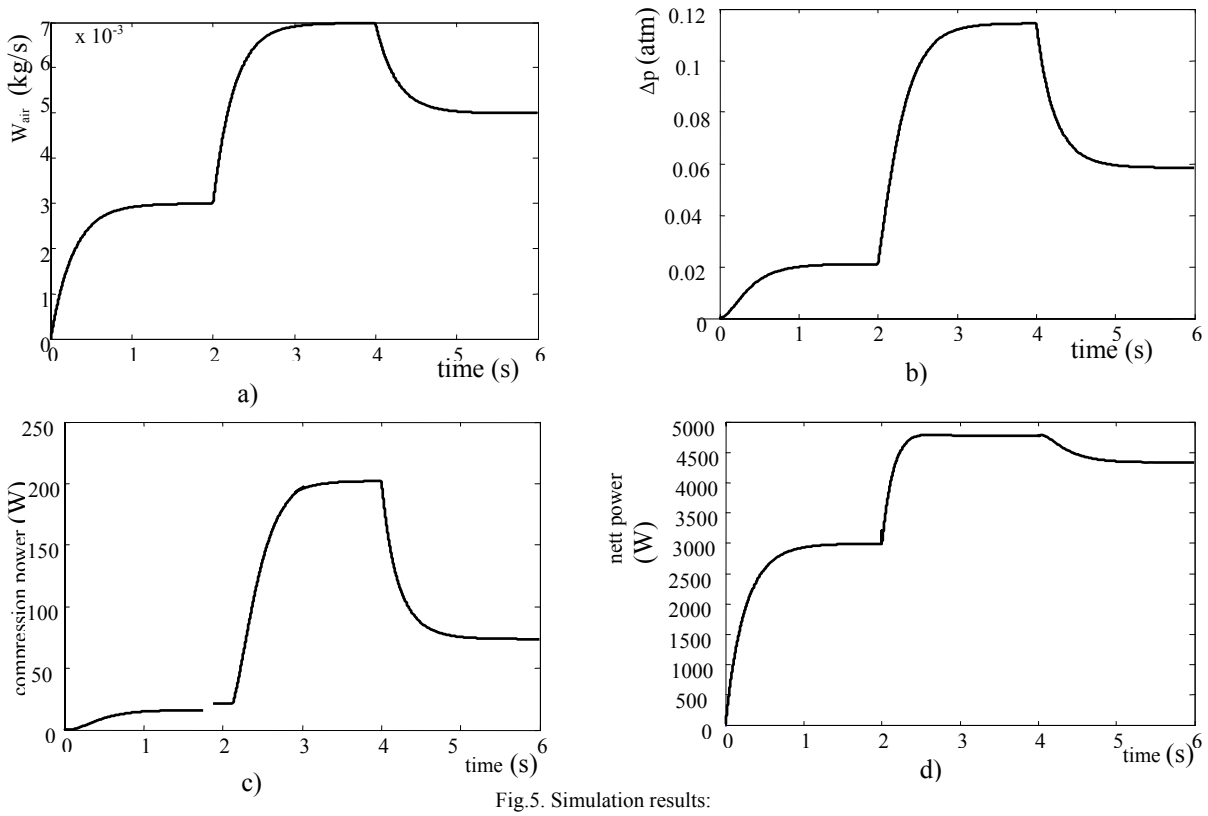

Fig.5. Simulation results:
a) mass air flow vs. time; b) air pressure vs. time c) compression power vs. time d) fuel stack net power vs. time.

VII. CONCLUSIONS

The model described in this article is from the empirical point of view approach. This model enables to simulate fuel cells *V–J* curves in typical conditions..

The analysis of the fuel cell performances allows concluding that:

- the empirical developed model of the fuel cell is easy to use for the simulation of the fuel cell operation;
- operate at low pressure balances the ratio between price of compression subsystem and performance for low density fuel cells stack;
- the developed blower model allows an easy approach for the simulation of the fuel cell/blower system;
- the study of the pressure loses in the channels permits to remark that for a cell active surface less than 400 cm² , a blower can compensate these loses;
- in this paper the authors have ignored the problem of the water and temperature management. The operating at low pressure influences the water and temperature management.
- high pressure allows an operation at high power density, which give a better ratio power/volume. A compressor is needed which is more expensive than a blower.

REFERENCES:

[1] Ph. Stevens, F. Novel-Cattin, A. Hammou, Cl. Lamy, M. Cassir, *Piles à combustible,* Techniques de l'Ingénieur, traité Génie électrique, Article D3340, Parution 08/2000.

[2] U.S. Department of Energy Office of Fossil Energy, National Energy Technology Laboratory Morgantown, West Virginia, *Fuel Cell Handbook (Sixth Edition)*, DOE/NETL-2002/1179, November 2002.

[3] T.A. Zawodzinski and al., Determination of water diffusion coefficients in perfluoro-sulfonate ionomeric membranes, *J. Phys. Chem*., vol. 95, (1991), 6040.

[4] J.C. Amphlett, R.M. Baumert, R.F. Mann, B.A. Peppley, P.R. Roberge, Performance modeling of the Ballard Marck IV solid polymer electrolyte fuel cell. I. Mechanistic model development*, J. Electrochem. Soc.*, Vol. 142, No. 1, January 1995.

[5] J.M. Corrêa, F.A. Farret, J.R. Gomes, M.G. Simões, Simulation of Fuel-Cell Stacks Using a Computer-Controlled Power Rectifier With the Purposes of Actual High-Power Injection Applications, *IEEE Trans. On Industry Applications*, VOL. 39, NO. 4, JULY 2003

[6] S. Busquet., C.E. Hubert, J. Labbé, D. Mayer, R. Metkemeijer, A new approach to empirical electrical modelling of a fuel cell, an electrolyser or a regenerative fuel cell, *Journal of Power Sources,* vol.134, (2004), 41–48.

[7] J.J. Baschuk, Xianguo Li, Modelling of polymer electrolyte membrane fuel cells with variable degrees of water flooding, *Journal of Power Sources*, vol. 86, 2000, 181–196.

[8] J. Kim, S. Lee, S. Srinivasan, Modeling of proton exchange membrane fuel cell performance with an empirical equation, *J. Electrochem. Soc.,* Vol. 142, No. 8, 1995, 2670–2674.

[9] C. Marr, X. Li, Composition and performance modelling of catalyst layer in a proton exchange membrane fuel cell, *Journal of Power Sources,* 77, 1999, 17–27.

[10] S. Maharudrayya, S. Jayanti., A.P. Deshpande, Pressure losses in laminar flow through serpentine channels in fuel cell stacks, *Journal of Power Sources,* vol. 138, (2004), 1–13.

[11] Sylvain Gelfi, Anna G. Stefanopoulou, Jay T. Pukrushpan, Huei Peng, Dynamics of Low-Pressure and High-Pressure Fuel Cell Air Supply System, *Proceedings of the 2003 American Control Conference*, Denver, CO, June, 2003.

[12] J.M. Mérigoux, Ventilateurs. Compresseurs. Notions fondamentales. Dimensionnement., Techniques de l'Ingénieur, traité Génie mécanique, Article B4500, 2000.

[13] AMETEK, Rotron, Technical & Industrial Products, Tech. Bulletin, 5.7" BLDC Bypass Blower, www.ametektmd.com\pdf.